Published by :
http://www.ijert.org

International Journal of Engineering Research & Technology (IJERT)
ISSN: 2278-0181
Vol. 9 Issue 01, January-2020

Diagnostics Assessment of Inter-turn Faults on Distribution Transformers Windings: Application of Sweep Frequency Response Analysis

J.O. Aibangbee
Department of Electrical/Electronic & Computer Engineering, Bells University of Technology, Ota, Ogun State, Nigeria

S.O. Ikheloa
Department of Electrical Technology, National Institute of Construction Technology, Uromi, Nigeria

***Abstract*:- This study presents in-depth diagnostics assessment of inter-turn faults on distribution transformers windings based on sweep frequency response analysis application. Measurements and experimental test were performed in high voltage laboratory with the measured frequency ranges from 100 Hz to1.0 MHz with 400 frequency points per decade using correlation coefficient and spectrum deviation as two statistical indicators for comparing the frequency responses. Results show that the performed experiments proved that the structure and shape of transfer function appears to be a function of the type, overall physical size and complexity of the transformer winding. The usage of correlation coefficient and spectrum deviation for comparison of the frequency responses obtained through SFRA measurements provides quantitative indicators of the fault presence on the transformer windings; the fault severity level in the shorted turns; and also in precisely detecting inter-turn faults along the transformer windings down to a few shorted turns on the winding. Measurements further proves that the voltage gain transfer function when measuring across a HV winding with other windings floating and not shorted is more sensitive to inter-turn winding faults; the deviation of the low frequency response of the LV winding located on the same phase of the damaged HV winding is large enough to indicate the fault occurrence; different levels of faults severity in the shorted turns with resistance values of 0 Ω, 2 Ω 4.4 Ω and 6.8 Ω causes differential current of 11.5%, 1.56%, 0.85% and 0.59% rated current under full load conditions of the transformer.**

Keyword*: *Correlation coefficient, Spectrum deviation, Transformer, inter-turn Faults, Windings, Sweep Frequency Response Analysis.

1. INTRODUCTION

Distribution or Power transformers are the most expensive and strategically important elements of any electrical power generation and transmission system. However, they do suffer from internal winding faults principally due to insulation failure; these faults must be quickly and accurately detected and the appropriate action taken to isolate the faulty transformer from the rest of the power system [1]. If not quickly detected, these faults can propagate and lead to catastrophic phase to ground or phase to phase faults resulting in a complete transformer breakdown which in turn generate substantial costs for repair or replacement and financial loss due to the power outage [2]. Most power utilities are therefore highly motivated to detect inter-turn short circuit fault in its earliest stage to prevent further damage to the transformer and electrical network. Conventional methods for early detection of failures in power transformers such as dissolved gas in oil analysis, partial discharge analysis and power factor tests, display considerable limitations in detection of inter-turn faults on the transformer windings [3]. Also the problem with the lastly developed power transformers assessment methods is that they just only give a general indication of the internal status of the transformer and do not permit the detection of inter-turn winding faults [4]. Frequency response analysis (FRA) as one of the well-recognized methods for on-site diagnosis of power transformers is based on the fact that every transformer winding has a unique signature of its transfer function which is sensitive to change in the parameters of the winding, namely resistance, inductance and capacitance.

Any geometrical or electrical changes within the transformer due to internal faults which have an effect on the capacitive or inductive behavior of a transformer winding cause a change in the transfer function of the winding and consequently a modification of its frequency response. FRA has been widely applied to power transformers to investigate mechanical integrity of the windings [5]. There are two ways for making frequency response analysis (FRA) measurements: Sweep frequency response analysis (SFRA) and low voltage impulse method (LVI). However, the second option is not considered in this article.

Given the potentials of sweep frequency analysis, [6] deals with development of a diagnosis approach based upon sweep frequency analysis, for detecting inter-turn winding faults. In recent years, applicability and sensitivity of the SFRA method in evaluating mechanical integrity of core, windings and clamping structures within power transformers has been extensively tested by means of faults simulations in laboratory and of real cases studies of transformers on site [7–13]. A literature review indicates that all of the contributions pertinent to the present study have concentrated only on inter- disk type faults and find it enough to show the overall changes of the frequency response of the transformer as a result of faults [14–18]. While the effects of the inter-turn faults are known to be problematic, the current study was focused upon obtaining a better understanding of the complex physical behavior of the transformer in the presence of inter-turn faults. Obviously, a correct understanding of what governs the modification of the physical behavior of the transformer as a result of inter-turn faults would assist in justifying the changes of winding frequency response and hence developing a reliable and sensitive fault detection method.

International Journal of Engineering Research & Technology (IJERT)
ISSN: 2278-0181
Vol. 9 Issue 01, January-2020

II. MATERIALS AND METHODS

2.0 SFRA MEASUREMENT

The SFRA method injects sinusoidal low voltage signals of varying frequencies into one side of the winding and measures the output signals as they exit the winding in order to obtain the winding transfer function. Treating a power transformer, undergoing SFRA, as a two-port network, the transfer function of the network is defined as the quotient of the output to input frequency responses when the initial conditions of the network are zero. Fig. 1 illustrates a basic SFRA measurement circuit including two-port network model of the transformer where Zij parameters in the model are formed by distributed resistive, capacitive, self and mutual inductive elements of the electrical equivalent circuit of the transformer. The tested impedance, in this case the impedance of the winding, is denoted by Z_{12}. In a case where the input and measured signals are generally referenced to ground; Z_{11} and Z_{22} represent the impedance paths to ground, through the bushing insulation. Z_{21} represents the impedance between the two references grounds which in practice approaches zero because the negative terminals in the above diagram are short-circuited through the transformer tank when the transformers is tested. Finally, S is the source used for generating the input sinusoidal signal and Z_S is the impedance of the source.

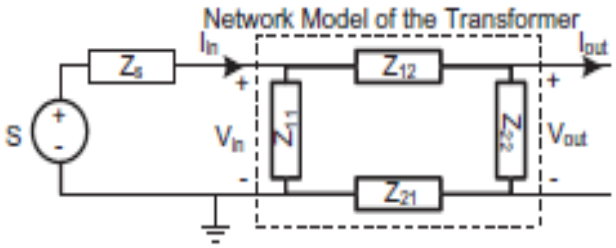

Fig.1: Basic SFRA measurement circuit including two-port network model of the transformer.

In this study, determination of the transfer function in the frequency domain was performed with a network-analyzer which used for generating the input sinusoidal signal, also making the voltage measurements and manipulating the results. Omicron measuring system was used in the measurements carried out in this paper. The tracking generator of the network-analyzer produced an alternating voltage of 5 V in amplitude as the reference signal of the measuring system. Two leads carrying input and output (test) signals were used for the connections between the network-analyzer and the bushings at two ends of the test winding. The transformer tank and the lead ground shields were connected together to assure that no external impedance is measured and also reduce the effect of noise and the environmental effects. This measurement setup accompanied by the experimental test object completes the test setup for performing the SFRA measurements. In the tests carried out in this study, the measured frequency range is 100 Hz–1 MHz with 400 frequency points per decade. The use of such high number of points which lead to increasing the taken time to make each measurement is justified by the decrease in the probability of missing true resonance points and losing resolution in the approximated transfer function with the collected data points. With the used sweep settings, an SFRA scan could take a few minutes.

2.1 Experimental Setup

SFRA measurements were carried out in high voltage laboratory on a three phase, two winding, 33 kV/415 V, 100 kV A distribution transformer with a turn ratio of 4550/60. The LV and HV windings of the transformer had layer and disk-type configurations respectively. Inter-turn faults were imposed on the turns of outermost layer of HV disks, which was the only accessible part of the transformer's windings. In order to develop inter-turn short circuit faults, in steps, the transformer oil was pumped out and the front wall of the transformer tank was removed to expose the windings. After the windings were allowed to dry, two conductors on the farthest layer of the second disk from the line end of the HV winding on phase **U** located at two ends of the layer, were chosen and the insulation over them at a point on each was carefully removed to make tapping points. The next step was extracting leads from the tapping points on the chosen conductors. Low impedance insulated wires were attached to the conductors by means of specific clamps embracing the conductors at the tapping points. The leads were then brought out of the transformer to allow easy access to the internal turns and also providing possibility for externally producing inter-turn faults. Since it was difficult to quantify exactly what number of turns involved by the fault, so after the connections were completed, the winding was energized by a low voltage power supply and the open circuit voltage between the tap conductors was recorded. This measured voltage between the taps, divided by the line to neutral value of the measured voltage applied to the winding, was an exact measure of the fraction of the winding that was involved by the fault. The fault level that could be realized by shunting the tap conductors was equal to 0.2% of the turns on the winding which involves a very small percentage of the winding.

Before reassembling the transformer, an insulation resistance test was performed to verify that the resistance of the tap conductors to ground was greater than 1 MΩ. A glass wall as a replacement for front wall of the transformer tank was fixed to the tank by screw bolts and then the oil refilled. Fig. 2 shows a physical view of the tested transformer before and after refilling the oil to the transformer tank. After reassembling of the transformer, inter-turn faults could be initiated by connecting two taps to each other through a low impedance knife switch to be able to handle the extremely high circulating fault currents flowing through the shorted turns. To adjust the fault severity in the shorted turns, a variable resistor was used in series with the switch in the conductive path between the terminals of the fault region. Various levels of fault severity can then be attained by changing the value of the fault resistance in this leakage path. The sketch in Fig. 3, illustrates an exaggerated presentation of the corresponding geometrical and circuit domain of the transformer coils and also the details of the tapping points and the initiated fault on phase **U** of the transformer HV winding.

International Journal of Engineering Research & Technology (IJERT)
ISSN: 2278-0181
Vol. 9 Issue 01, January-2020

(a)

Fig.2. (a) Front view of the tested before refilling the oil

(b)

(b) Side view of the transformer after refilling the oil.

In the figure, the external limiting fault resistance and the time controlled switch for initiating the fault are denoted by **"S"** and **"Rf**" symbols respectively.

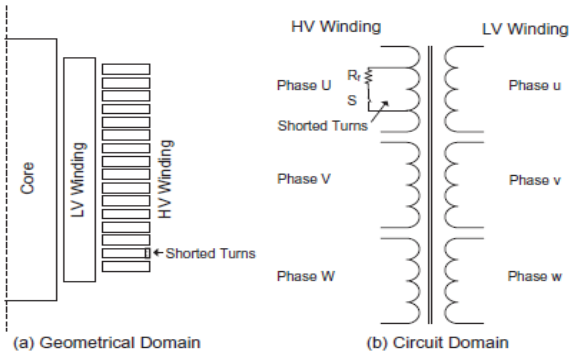

Fig.3. Exaggerated transformer coils and the initiated fault on the 2nd disk of the HV winding on phase ''U''

A close view of the considered transformer's HV windings and tap positions of the introduced fault, before and after refilling the oil to the transformer tank, is given in Fig. 4

Before conducting the experiments, a full-load test was performed on the transformer with the taps open to verify that the modifications had not changed the transformers' normal operating characteristics. Once this test was completed, selected fault scenarios can be initiated to make the SFRA measurements.

(a) Before refilling the oil

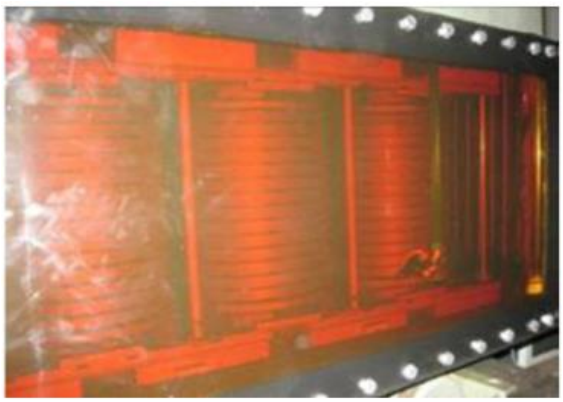

(b) After refilling the oil to the tank.

Fig. 4: Tap positions along the HV winding of the transformer.

Efforts were made by the authors in order to identify the most appropriate configuration for making sensitive frequency response measurements. Two different transfer functions, various terminal configurations and three categories of measurement types were studied. The sensitivity of the two transfer functions, i.e. voltage gain and impedance, was investigated by analyzing the frequency responses determined by each of the methods. Once the appropriate transfer function for fault detection was identified, the next step was to determine the most appropriate combination of terminal connection and measurement type for achieving the maximum fault detection ability. Open and short circuit terminal configuration and three categories of winding measurement including high voltage, low voltage and inter-winding measurements were made to identify the most sensitive configuration for detecting winding faults. Through these studies, it was found that measuring voltage gain across HV winding of the transformer, keeping all HV and LV non-tested terminals floating, offers greater sensitivity and ability in fault detection, owing to preparing more number of resonance points and also effectively taking into account the core effects at lower frequencies.

Statistical parameters such as: correlation coefficient, spectrum deviation and maximum absolute difference have been proposed by [19–23] in order to establish the differences between recording of the SFRA measurements. Correlation coefficient and spectrum deviation as two statistical indicators were used in this study for comparing the SFRA

International Journal of Engineering Research & Technology (IJERT)
ISSN: 2278-0181
Vol. 9 Issue 01, January-2020

graphs. The corresponding mathematical expression of these parameters are given by

$$\rho = \frac{\sum_{i=1}^{n} x_i y_i}{\sqrt{\sum_{i=1}^{n} x_1^2 \sum_{i=1}^{n} y_i^2}} \quad (1)$$

$$\sigma = \frac{1}{n}\sum_{i=1}^{n}\sqrt{\left(\left[\frac{x_i - (x_i + y_i/2}{(x_i + y_i)/2}\right]^2 + \left[\frac{x_i - (x_i + y_i/2}{(x_i + y_i)/2}\right]^2\right)} \quad (2)$$

Where X(x_1, x_2, , , x_n) and Y(y_1, y_2, , ,y_n) are two set of n numbers, ρ is the correlation coefficient and σ is the spectrum deviation between these two sets. In investigating the relationship between the two signals, the highest possible similarity level is obtained by correlation coefficient equal to unity and spectrum deviation to zero. Table 1 shows the correlation and spectrum deviation between the faulted and non-faulted responses of phase **U** of the HV winding, calculated in decade frequency bands. The calculated indicators given in Table 1 are corresponding to the measurements which are shown in Fig. 5. In complete agreement with the measured graphs in Fig. 5, it can be clearly seen from the table that the largest deviation or smallest correlation values are related to the lowest frequency band of the responses, i.e. 100 Hz–1 kHz, which is much affected by the inter-turn fault. Also, the upper zero values of the spectrum deviation and under unity values of the correlation coefficient in the 1–10 kHz and 10–100 kHz frequency bands indicate the differences between the faulted and non-faulted responses at medium frequencies. From the table, the indicators illustrate good agreement between the responses from 100 kHz up to 1 MHz which proves that the high frequencies are not affected by the inter-turn fault. Table 1 show the correlation and spectrum deviation between faulted and Non-faulted responses of phase U of the HV winding. Comparing the corresponding values of the two considered indicators in Table 1 proves the higher sensitivity and reliability of the spectrum deviation as a statistical indicator in detecting inter-turn faults.

Table 1: Correlation and spectrum deviation between faulted and Non-faulted responses of phase U of the HV winding

Frequency Decade	ρ	σ
100 Hz-1kHz	0.9951	0.1204
1-10 kHz	0.9968	0.0434
10-100 kHz	0.9983	0.0342
100 kHz -1 MHz	0.9998	0.0068

Table 2: Correlation and spectrum deviation between faulted and non – faulted responses of three phases of the HV winding for a fault on phase U

Frequency Decade	Phase U		Phase V		Phase W	
	ρ	σ	ρ	σ	ρ	σ
100 Hz-1kHz	0.9951	0.1204	0.9991	0.0281	0.9985	0.0170
1-10 kHz	0.9968	0.0434	0.9995	0.0193	0.9968	0.0326
10-100 kHz	0.9983	0.0342	0.9994	0.0178	0.9994	0.0130
100kHz -1 MHz	0.9998	0.0068	0.9999	0.0031	0.9999	0.0024

Table 3: Correlation and spectrum deviation between normal and faulty responses of phase U taken by HV, LV and inter-winding measurements

Frequency Decade	HV		LV		INTER-WINDING	
	ρ	Σ	ρ	σ	ρ	σ
100 Hz-1kHz	0.9951	0.1204	0.9817	0.6040	0.9999	0.0010
1-10 kHz	0.9968	0.0434	0.7721	0.4625	0.9997	0.0119
10-100 kHz	0.9983	0.0342	0.9943	0.0866	0.9985	0.0254
100kHz -1 MHz	0.9998	0.0068	0.9999	0.0029	0.9999	0.0011

Table 2 shows the correlation and spectrum deviation between the faulted and non-faulted responses of three phases of the transformer HV winding, corresponding to the graphs shown in Figs. 5, 7 and 8. Table 3 illustrates the results of applying the indicators to the normal and faulty responses of phase **u** of the transformer taken by HV, LV and inter-winding measurements. Table 4 shows the correlation and spectrum deviations between the baseline measurement of the phase **U** of HV winding and four measurements made during the fault occurrence with different severity levels on the same winding.

Table 4: Correlation (ρ) and spectrum deviation (σ) between normal and faulty phase U of HV winding Faults with different severity levels

Frequency Decade	Fault Impedance (R_f)			
	6.8Ω		4.4 Ω	
	ρ	σ	ρ	σ
100 Hz-1kHz	0.9987	0.0257	0.9981	0.0349
1-10 kHz	0.9998	0.0050	0.9997	0.0078
10-100 kHz	0.9997	0.0142	0.9995	0.0181
100kHz-1 MHz	0.9998	0.0049	0.9999	0.0056
Frequency Decade	Fault Impedance (R_f)			
	2.0Ω		0.0Ω	
	ρ	σ	ρ	σ
100 Hz-1kHz	0.9968	0.0560	0.9951	0.1204
1-10 kHz	0.9991	0.0149	0.9968	0.0434
10-100 kHz	0.9992	0.0244	0.9983	0.0342
100kHz-1 MHz	0.9998	0.0065	0.9998	0.0068

III. ANALYSIS AND RESULTS

In order to obtain diagnosis criteria for detecting of inter-turn winding faults, a fault involving 0.2% turns was initiated on the phase **U** of HV winding of the transformer. The imposed fault involves a very small percentage of the winding. The smallest value of the fault resistance was chosen to account for a metal-to-metal contact and dispose of an extreme value which helped to evaluate trends. Over the course of the experimental tests, series of experiments were conducted to verify the correctness of the measurement records. Fig. 5 depicts two graphs collected in normal and faulty operating conditions of the transformers when the transformer is filled with oil. It is clear from the results, that the faulted response is substantially different from the non-faulted response over the low frequency range below 1 kHz. When a short circuit occurs at a given turn, the voltage is forced to drop in it and consequently circulating current flows in the short circuited turn, to limit the entering flux into the turn. Considering an ideal situation where a turn with null resistance is short-circuited by a null fault resistance. In this condition, the shorted turn would have a null voltage at its terminals and hence no flux would enter inside its contour. The larger the fault resistance, the larger is the flux entering inside the turn.

International Journal of Engineering Research & Technology (IJERT)
ISSN: 2278-0181
Vol. 9 Issue 01, January-2020

On the contrary, as the severity of the short circuit increases, means that the turns short-circuited with smaller fault resistance, a larger amount of flux would be surrounding the shorted turns.

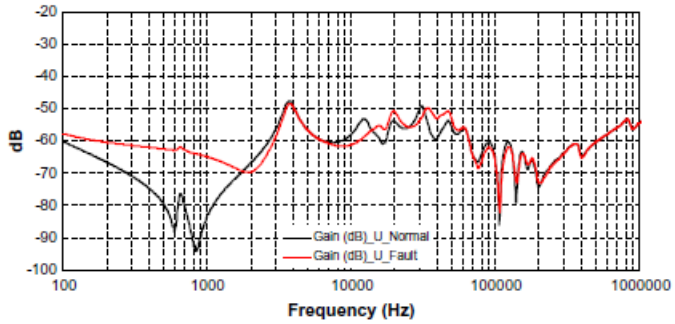

Fig. 5: Transfer function for phase U of the HV winding in normal and faulty operating conditions of the transformers

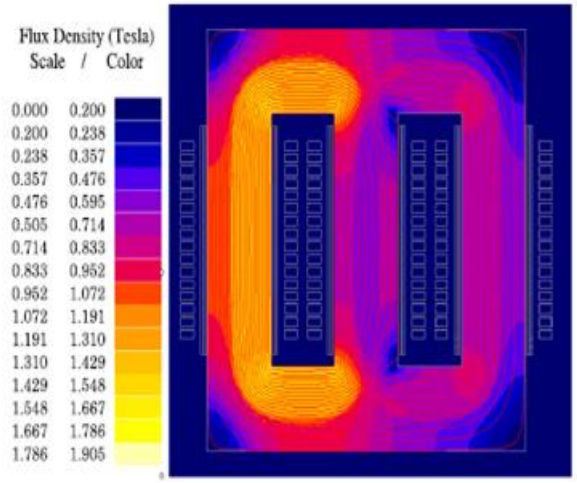

(a)
Electromagnetic flux distribution under normal operating condition

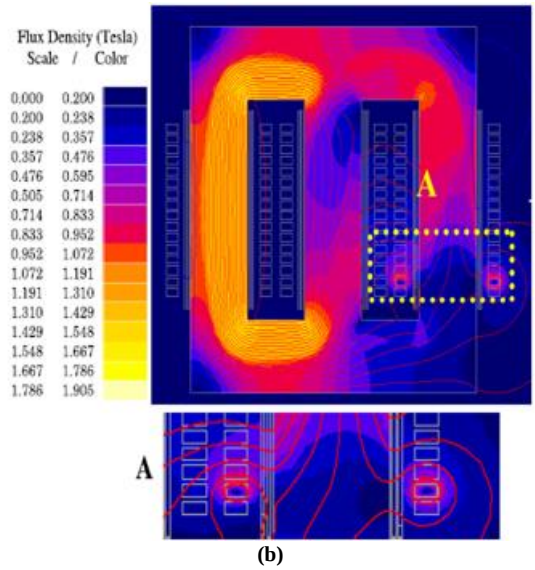

(b)
Electromagnetic flux distribution due to short circuit fault along the 2nd disk from the line end of the HV winding on phase U

Fig. 6: Flux plot of the transformer under normal and faulty operating conditions.

Flux plot and color shaded plot of the electromagnetic flux density inside the studied transformer under normal operating condition and after a short circuit fault occurs along one of the transformer HV winding's disks on phase **U**, with a fault resistance equal to 1m**Ω**, are given in Fig. 6a and 6b respectively. It can be clearly seen from Fig. 6, how the distribution of the magnetic flux is fundamentally altered after the fault occurrence on the winding. There is a strong leakage flux, despite the normal leakage flux, surrounding the damaged turns through air paths and reduced flux lines inside the shorted turns on the core limb due to the fault occurrence. Dense flux trajectories outside the faulty region in Fig. 6b correspond to higher levels of flux density, outside the damaged turns and reduction of it on the transformer core limb as it can be clearly identified in color shaded plot of the electromagnetic flux density.

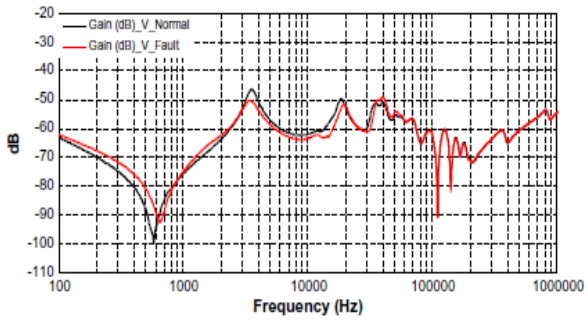

Fig.7: Frequency response of phase V before and after faults on phase U of the HV winding

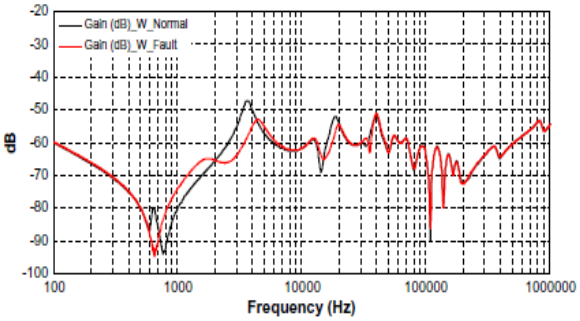

Fig.8. Frequency response of phase W before and after faults on phase U of the HV winding

By considering all these observations, one can conclude that the winding short circuit fault changes the magnetizing characteristics of the transformer core which in turn causes the low-frequency deviation of the winding frequency response. The core effect is located in the lowest frequency bandwidth on the winding frequency response, when measuring across a winding with other windings floating and not shorted. Inter-turn faults, in addition to the changes at lower frequencies of the frequency response, also will give differences at mid-frequencies. In a range of 10 kHz up to 100 kHz the differences are very significant.

As can be seen from the response graphs in Fig. 5, the general effect of the inter-turn fault is a shift of the transfer function towards higher frequencies. The movement of the resonant frequency points to the right on the response plot as a result of inter-turn fault occurrence is much more obvious in the frequency range of 10 kHz up to 60 kHz. Trends of increasing and decreasing absolute values of the response are

International Journal of Engineering Research & Technology (IJERT)
ISSN: 2278-0181
Vol. 9 Issue 01, January-2020

also detectable in this frequency range. A closer look at the transfer function plot in Fig. 5 indicates that the magnitude of the transfer function changes as much as 6 dB in the pronounced mid-frequency resonance at around 38 kHz from the faulty case where the fault resistance is almost equal to zero to the normal response. This absolute effect is comparable to the uncertainty of the measurement. There is a linguistic agreement between some experts, that any difference within about 0.2 dB from one set of SFRA measurements to the next is usually considered as an indication of a physical change inside the transformer. The normal and faulty traces are almost identical at all frequencies above approximately 100 kHz where traces overlay very well in this range. It should be noted that although the influence of the fault on the faulted phase response is much more obvious; but the differences of the two other phases responses as a result of fault occurrence is noticeable too. Figs. 7 and 8 present the frequency responses of phases **V** and **W** of the transformer HV winding in both normal and faulty operating conditions, retaining the same fault case considered above. Again a same type of behavior similar to the faulted phase response, i.e. movement of the transfer function to higher frequencies and changing the absolute values of the transfer function, is observed for the responses of failure-free phases. Albeit, as compared to faulted phase response which the effect of the inter-turn fault reaches into the midrange of the frequency response up to 100 kHz, Fig. 5, the effect of the fault is negligible above 60 kHz for Phase **V** and 25 kHz for phase **W** in their corresponding frequency responses. The effect of the fault on the low frequency range of the responses of non-faulted phases is seriously different. Figs. 7 and 8 reveal that, except removing one of the core resonance points of phase **W**, there is not any other serious modification in the low frequency responses of the non-faulted phases in spite of the drastic change in the low frequency range of the faulted phase response. Obviously this behavior is a result of the limitation of the fault effects on the core limb corresponding to the damaged winding of the transformer.

The results in Table 4 illustrate how the spectrum deviation of the faulty responses with the baseline measurement increases with increasing of the fault severity in the shorted turns. In order to prove the characteristic signatures attained to inter-turn faults inferred based on the inspection of transfer function of the winding in faulty and normal operating conditions, additional experiments were performed with different levels of the fault severity in the shorted turns. As indicated in Table 4 and Figs. 9–11, it should be noted that the faults with resistance values of 0 Ω, 2 Ω 4.4 Ω and 6.8 Ω cause a differential current of only 11.5%, 1.56%, 0.85% and 0.59% rated current respectively under full load conditions of the transformer which makes detection of theses fault by traditional transformer protection devices to a very challenging task. The measurements performed proves that the voltage gain transfer function when measuring across a HV winding with other windings floating and not shorted is more sensitive to inter-turn winding faults. In addition, the deviation of the low frequency response of the LV winding located on the same phase of the damaged HV winding is large enough to indicate the fault occurrence. It is also proved that the inter-winding measurement is less effective in detecting inter-turn faults as compared to the two other HV and LV categories. Figs. 9–11 show the magnitude plot of the transfer functions corresponding to three phases of the transformer HV winding obtained from a frequency sweep analysis as a result of 0.2% winding short circuit on phase **U** but with different fault resistance values to create the desired fault severity level in the shorted turns. It proves that the main characteristic features associated with inter-turn faults extracted from the frequency response measurements, namely displacement of the resonant frequency points to the right and a change in the transfer function magnitude are discernible for all the fault severity levels in the mid-frequency range of three phase frequency responses. Furthermore, the change in the low frequency response of the faulted phase is clearly noticeable for all the fault severity levels.

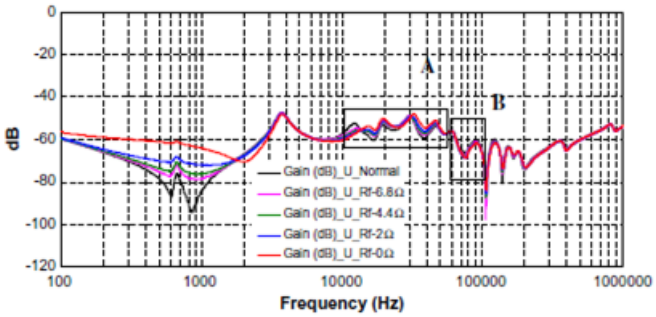

Fig 9: (a)

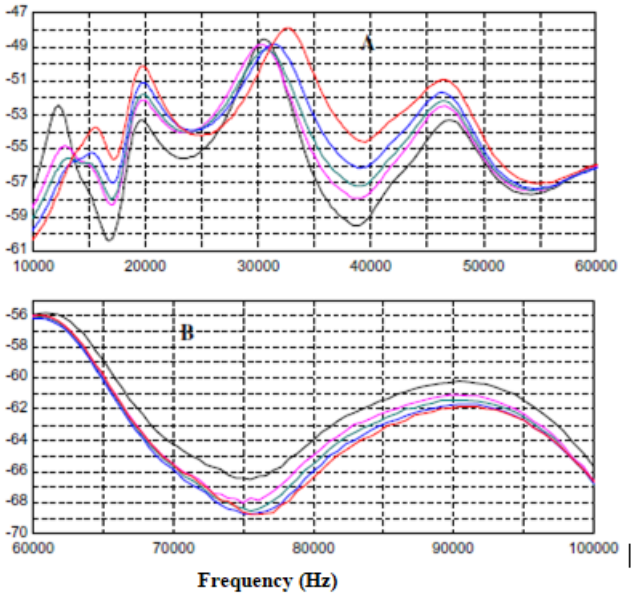

(b)

Fig. 9: (a) and (b) Normal and faulty phase U of the HV winding with different fault severity levels

International Journal of Engineering Research & Technology (IJERT)
ISSN: 2278-0181
Vol. 9 Issue 01, January-2020

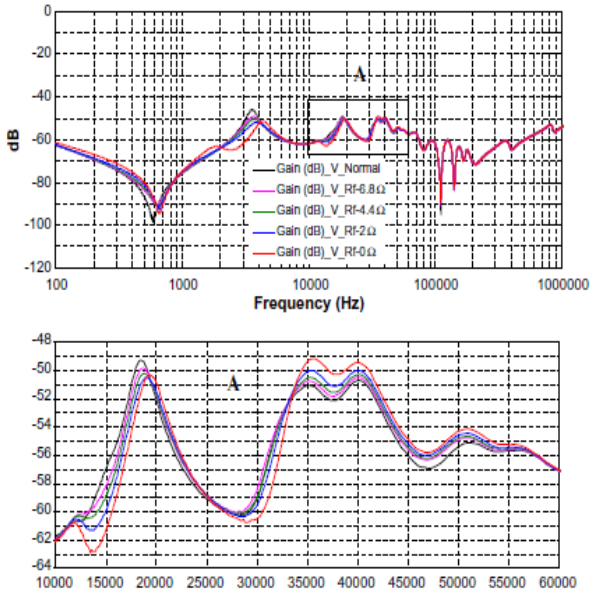

Fig. 10: Response of phase V, before and after fault with different severity levels on phase U of the HV winding.

Table 3 illustrates the results of applying the indicators to the normal and faulty responses of phase **u** of the transformer taken by HV, LV and inter-winding measurements. The corresponding measurement results are shown in Figs. 5, 12 and 13. The spectrum deviation for the responses related to the LV winding reaches high values in the 100 Hz–1 kHz and 1–10 kHz decade bands, where the changes caused by the inter-turn fault are most apparent. The spectrum deviation between results from inter-winding measurement is very close to zero throughout all the frequency bands. This is a good indication of less sensitivity of inter-winding measurement in detecting inter-turn faults. Fig. 12 illustrates the frequency response of phase **u** of the transformer LV winding before and after inter-turn fault occurrence on phase **U** of the HV winding. It can be clearly seen that the most important feature in regard of diagnosis is the deviation of the low frequency response of the transfer function and also creation of one new resonance point around 20 kHz as a result of fault occurrence.

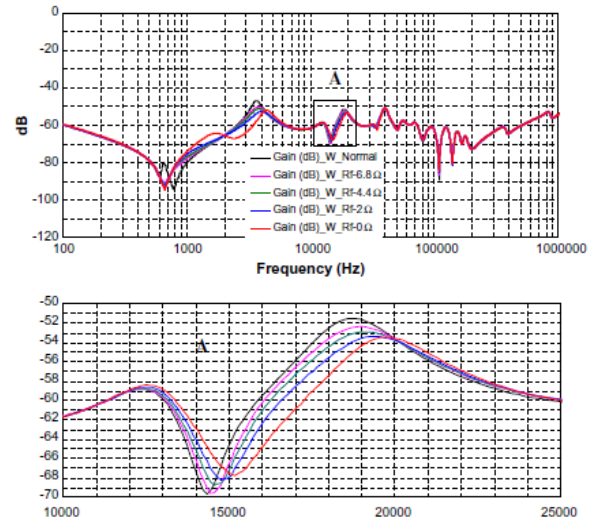

Fig. 11: Phase W, before and after fault with different severity levels on phase U of the HV winding

Modification of the low frequency response of phase **u** of the LV winding is justified by this fact that this winding is located on the same core limb which the damaged HV winding on phase **U** is located on it, so both the responses of the LV and HV windings are affected by modifications of the core in the fault region.

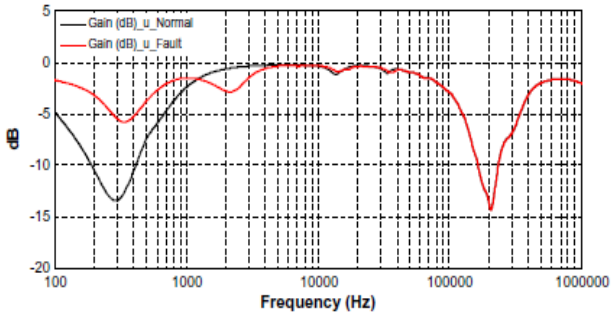

Fig. 12: Normal LV winding of phase u Versus HV winding fault on phase U

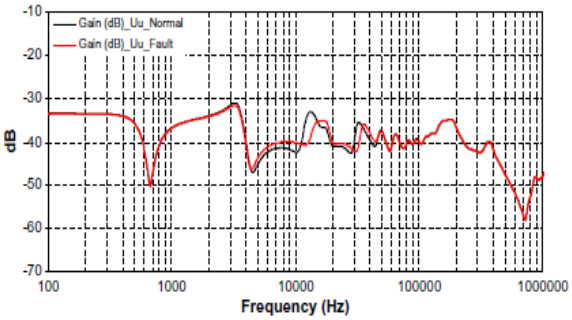

Fig. 13: Inter-winding measurement of phase U Versus HV winding fault on phase U.

The comparison of HV and LV winding measurements in Figs. 5 and 12, indicates that contrary to HV winding measurements, which the effects of inter-turn fault reach into the midrange of the frequency response up to 100 kHz, in LV winding measurements, high frequencies above 40 kHz are not affected by the fault. Fig.13 shows the SFRA results, taken by inter-winding measurements having the terminal of phase **U** of the HV winding as input and the corresponding terminal on the phase "u" of the LV winding as output, prior to and after inter-turn fault occurrence on the phase **U** of the HV winding. While reviewing the graphs from left to right, a partial difference is seen between normal and faulty responses starting from just above 10 kHz and continuing to around 45 kHz in the form of shifting the resonance points to the right and changing the absolute values of the transfer function. However there is not a visible fault indication in the low frequency range of the transfer function which looks very different to the HV and LV winding measurements. The low frequency deviation in the winding response as a result of inter-turn fault is governed by the interaction between core and windings while the inter-winding measurement is made with almost no reference to the core effects at lower frequencies.

IV. DISCUSSION

The SFRA is a method by which evaluation of the transformer condition is carried out by comparing an actual set of SFRA results to reference results. The experiments

International Journal of Engineering Research & Technology (IJERT)
ISSN: 2278-0181
Vol. 9 Issue 01, January-2020

presented provide the capability of the SFRA method as a diagnostic tool to detect inter-turn winding faults. According to the applied tests the sensitivity of the SFRA method can recognize an inter-turn fault involving 0.2% of turns on the transformer winding. The following points can be summarized. Measuring voltage gain across the HV winding of the transformer constitute the appropriate pair of system function and measurement type, because of preparing the maximum number of natural frequencies and so significantly improving the achievable sensitivity. Inter-turn faults along the winding will cause significant changes in the magnetic behavior of the transformer and hence give deviation in the low frequency range of the frequency response where it is much affected by the magnetic core. In the experiment carried out in this paper on a distribution transformer, some useful characteristic signatures associated with inter-turn faults were extracted from the measurement records in order to obtain diagnosis criteria for detecting winding inter-turn faults. As seen in Table 1, all the correlation values are acceptably around unity in all the frequency bands, however the value of the spectrum deviation in the 100 Hz–1 kHz band is large enough to indicate the inter-turn fault occurrence. Table 2 shows the correlation and spectrum deviation between the faulted and non-faulted responses of three phases of the transformer HV winding, corresponding to the graphs shown in Figs. 5, 7 and 8. It is seen from the table that the largest differences between the faulted and non-faulted graphs are clearly related to the damaged phase U. The corresponding values of the undamaged phases of the transformer HV winding, i.e. **V** and **W** phases show a similar trend to the damaged phase throughout all the frequency bands. However, the lower values of the spectrum deviation coefficients for the undamaged phases as compared to the corresponding value of the damaged phase in the same frequency bands, amounts to a reduced effect of the fault on the non-damaged phases. Table 3 illustrates the results of applying the indicators to the normal and faulty responses of phase **u** of the transformer taken by HV, LV and inter-winding measurements. The corresponding measurement results are shown in Figs. 5, 12 and 13. The spectrum deviation for the responses related to the LV winding reaches high values in the 100 Hz–1 kHz and 1–10 kHz decade bands, where the changes caused by the inter-turn fault are most apparent. The spectrum deviation between results from inter-winding measurement is very close to zero throughout all the frequency bands. This is a good indication of less sensitivity of inter-winding measurement in detecting inter-turn faults.

As seen, the use of statistical coefficients of the SFRA records provides quantitative way for diagnosing the presence of a fault, complementing the qualitative approaches. In addition to the benefits gained from adding more objectivity and transparency to interpretation of the SFRA results, significant advantages would accrue by quantifying the fault severity level through the use of coefficients. The results in Table 4 illustrate how the spectrum deviation of the faulty responses with the baseline measurement increases with increasing of the fault severity in the shorted turns. It has to be highlighted that the reliability of the fault diagnosis is achieved by means of the qualitative approach based on the detection of the characteristic patterns that appear in the frequency response of the windings during the fault occurrence. Once the fault is identified, the computation of the statistical coefficients allows the quantification of the degree of fault. The performed experiments in this study proved that the structure and shape of transfer function appears to be a function of the type, overall physical size and complexity of the transformer winding. The correlation coefficient and spectrum deviation were used to calculate the amount of agreement or disagreement between the two sets of faulty and normal measurements for quantitative explanation of the fault presence on the transformer windings. Spectrum deviation was found to be more effective than correlation coefficient in establishing the differences between the recordings of the SFRA measurements.

V. CONCLUSIONS

Successful operation of SFRA method in precisely detecting inter-turn winding faults with a sensitivity of better than 0.2% of turns along the winding, was performed on a real distribution transformer. A method which assures sufficient reproducibility of the SFRA measurements was explained. The experiments on a distribution transformer for estimating the sensitivity of different transfer functions in detecting of inter-turn faults were discussed. It was found through the experiments that the voltage gain measurement across the HV winding of the transformer with other windings floating and not shorted is the most appropriate configuration for detecting inter-turn faults along the windings. Also, the low frequency measurements proved to be very helpful for accurately monitoring the health condition of the transformer windings. Statistical indicators were used to support the interpretation of the SFRA results, and also quantifying the discriminative features associated with the inter-turn faults. The spectrum deviation and correlation coefficient proved to be effective tools to provide quantitative ways for diagnosing and, at the same time, to quantify the degree of the fault severity in the shorted turns. It was found that the differences between the normal and faulty responses of the transformers windings damaged by inter-turn faults, was more reflected in the spectrum deviation as compared to the correlation coefficient. Based on the findings, the SFRA method can provide effective interpretation of transformer performance, in terms of early fault detection.

REFERENCES

[1] Aggarwal RK, Mao P. (1998) “Digital simulation of the transient phenomena in high voltage power transformers with particular reference to accurate fault detection”. Internal conference on SIMULATION, conference publication no.457, IEE 1998, p. 390–7.

[2] Vahedi Abolfazl, Behjat Vahid (2011). “Online monitoring of power transformers for detection of internal winding short circuit faults using negative sequence analysis” Eur Trans Electric Power; 21(1):196–211.

[3] Behjat Vahid, Vahedi Abolfazl. (2011) A DWT-based approach for detection of interturn faults in power transformers. COMPEL: The International Journal Computer Math Electrical Electronics Eng; 30(2):483–504.

[4] Georgilakis PS. (2011) “Condition monitoring and assessment of power transformers using computational intelligence”. International Journal Electrical Power Energy System, vol. 33(10) London: Springer; p. 1784–5.

International Journal of Engineering Research & Technology (IJERT)
ISSN: 2278-0181
Vol. 9 Issue 01, January-2020

[5] Dickson EP, and Erven CC. (1978) "Transformer diagnostic testing by frequency response analysis" IEEE Trans Power Apparatus System; PAS-97(6):2144–53.

[6] Behjat Vahid, Vahedi Abolfazl, Setayeshmehr Alireza, Borsi Hossein, Gockenbach Ernst. (2011) "Diagnosing shorted turns on the windings of power transformers based upon online FRA using capacitive and inductive couplings. IEEE Trans Power 26(4):2123–33.

[7] Sweetser C, and McGrail T. (2003) "Sweep frequency response analysis transformer applications" A technical paper from doble engineering.

[8] Secue JR, and Mombello E. (2008) "Sweep frequency response analysis (SFRA) for the assessment of winding displacements and deformation in power transformers" Electric Power System Res; 78(6):1119–28.

[9] Leibfried T, and Feser K.(1999) " Monitoring of power transformers using the transfer function method". IEEE Trans Power Del. 14(4):1333–41.

[10] Feser K, Christian J, Neumann C, Sunderman U, Leibfried T, Kachler A. (2000) "The transfer function method for detection of winding displacements on power transformers after transport, short circuit" CIGRE paper 12/33-04.

[11] Wang M, John Vandermar A, Srivastava KD. (2005) "Improved detection of power transformer winding movement by extending the FRA high frequency range". IEEE Trans Power, 20(3):1930–8.

[12] Rahimpour Ebrahim, Christian Jochen, Feser Kurt, and Mohseni Hossein (2003) "Transfer function method to diagnose axial displacement and radial deformation of transformer windings" IEEE Trans Power, 18(2):493–505.

[13] Florkowski Marek, Furgal Jakub. (2009) "Modelling of winding failures identification using the frequency response analysis (FRA) method" Electric Power System Res 79(7):1069–75.

[14] Pleite Jorge, González Carlos, Vázquez Juan, and Lázaro Antonio.(2006) "Power transformer core fault diagnosis using frequency response analysis". IEEE MELECON, Benalmádena (Málaga) p. 1126–9.

[15] Christian J, Feser K, Sunderman U. (1999) "Diagnostics of power transformers by using the transfer functions method". Proceedings of IEEE international symposium on high voltage engineering, conference publication no. 467; p. 37–40.

[16] Islam Syed Mofiml.(2000) "Detection of shorted turns and winding movements in large power transformers using frequency response analysis. IEEE PES, winter meeting, vol. 3, Singapore; p. 2233–8.

[17] Islam S, and Ledwich G. (1996) "Locating transformer faults through sensitivity analysis of high frequency modeling using transfer function approach. In: Proceedings of IEEE international symposium on electrical insulation, Montreal, Quebec, Canada p. 38–41.

[18] Satish L, and Sahoo Subrat K. (2009) "Locating faults in a transformer winding: an experimental study". Electric Power System Res 79 (1):89–97.

[19] McGrail Tony,and Sweetser Charles.(2003) "Experiences with SFRA for transformer diagnostics. A technical paper from doble engineering

[20] Ryder SA. (2002) "Methods of comparing frequency response analysis measurements" Proceedings of IEEE international symposium on electrical insulation, Boston, Massachusetts; p. 187–90.

[21] Nafar Mehdi, Niknam Taher, and Gheisari Amirhossein. (2011) "Using correlation coefficient for locating partial discharge in power transformer" International Journal Electric Power Energy System; 33 (3):493–9.

[22] Vahidi B, Ghaffarzadeh N, and Hosseinian SH. (2010) "A wavelet-based method to discriminate internal faults from inrush currents using correlation coefficient". International Journal Electric Power Energy System; 32(7):788–93.

[23] Kumbhar Ganesh B, and Mahajan S. M. (2011) "Analysis of short circuit and inrush transients in a current transformer using a field-circuit